Selective laser-induced breakdown of xenon

V. E. Peet
Institute of Physics, Estonian Academy of Sciences, Riia 142, Tartu EE2400, Estonia
(Received 20 September 1994; revised manuscript received 5 December 1994)

Selective excitation of laser-induced breakdown of xenon by nanosecond laser pulses in the spectral range of 420–600 nm and light intensity of 10^{11} W/cm^2 has been studied. A number of multiphoton resonances have been identified in the breakdown excitation spectra and the excitation conditions within the focal volume have been determined from the ac Stark shift of the resonances. It has been shown that the breakdown initiation is influenced by odd harmonics of the laser light, which are generated in the focal volume. The phase-matched harmonic field induces the breakdown near some of the multiphoton resonances, while this field is able to suppress the breakdown under on-resonance excitation due to destructive interference between optical transitions. Taking into account the internally generated harmonics of the laser field, the interpretation of some of the previous experimental results is reconsidered.

PACS number(s): 32.80.Rm, 32.90.+a, 42.50.Hz, 52.50.Jm

I. INTRODUCTION

Laser-induced breakdown of a gas ("laser spark") is a well-known phenomenon associated with high-power lasers. In many applications of intense laser pulses the breakdown is an undesirable parasitic effect, which changes the properties of the gaseous medium and disturbs the propagation of the pulse. Thanks to extensive investigations of this phenomenon, the general picture of the processes leading to a breakdown has been understood rather well (see, e.g., [1–3]). For nanosecond laser pulses the initial electrons are created by the multiphoton ionization of gas atoms. Further, the photoelectrons gain energy from the laser field and produce an additional avalanche ionization which can lead to a complete ionization of the gas. It is clear that multiphoton ionization, as the beginning stage of these processes, plays a crucial role in the breakdown initiation.

The breakdown threshold can be reduced remarkably by the presence of intermediate excited states of gas atoms or molecules due to resonantly enhanced multiphoton ionization (REMPI). Already in the earliest experiments a significant dependence of the breakdown threshold on the laser wavelength was observed [4]. By using a tunable dye laser, Damany *et al.* [5] studied the breakdown near the three-photon resonance with the $6s$ excited state of xenon, where a number of four-photon atomic resonances were identified in the breakdown excitation spectra. Such a possibility of initiating a breakdown selectively is remarkable for a number of reasons. Selective breakdown visualizes the ionization channels and this method can serve in the study of multiphoton processes for the conditions where it is difficult to carry out the commonly used measurements of the ionization yield (laser-induced damage of the gas, high pressure, electronegative gases, etc.). Besides, the excitation of a selective breakdown allows one to study the breakdown itself, i.e., to study the processes in the focal volume, which are responsible for the breakdown initiation and determine the resistance of a gas against the laser-induced damage.

The present article describes experimental results of a selective excitation of a breakdown in xenon. These experiments were aimed at the study of the main channels of REMPI and other associated processes responsible for the initiation of a selective breakdown in a dense gas.

II. EXPERIMENT

A schematic diagram of the experimental setup is shown in Fig. 1. The breakdown of xenon was initiated by a tunable dye laser VL-22 pumped by an excimer XeCl laser. The dye laser had a two-stage amplifier and a Hänsch-cavity oscillator with a beam expander and a grating with 1200 grooves/mm. The spectral width of the dye laser output was 0.005 nm (full width at half maximum) and the energy of the laser pulse was 1–4 mJ per shot in the 420–600 nm spectral region.

The gas cell was made of stainless steel and contained xenon of 99.999% purity. Four quartz windows of the cell allowed one to focus the laser beam at different excitation geometries and detect the emission of laser-produced plasma. The plasma emission was collected by a quartz lens and measured by a photodiode and a charge-sensitive radiometer. A convenient glass filter was used to block the scattered laser light. The time-integrated signal from the radiometer was recorded on the x-y plotter.

Two excitation geometries were used to initiate the breakdown. In a unidirectional geometry the laser beam was focused into the gas by either a high-quality achromatic objective with the focal length f=50 mm or a spherical mirror with f=30 mm. In the excitation by counterpropagating beams the laser output was first focused into the cell by the objective and then retroreflected on itself by the spherical mirror with the overlapping of both beam waists. Formally, when the beam was focused by the on-axis spherical mirror alone, the excitation geometry was a counterpropagating one as well. In this case, however, the light intensity in the focal region

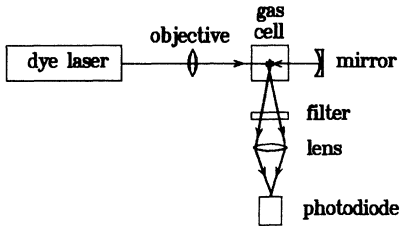

FIG. 1. Schematic diagram of the experimental setup.

of the reflected beam was several orders of magnitude larger than the intensity of the counterpropagating unfocused beam. All the effects related to the excitation by counterpropagating beams need both the incident and the reflected beam to be focused and these effects are extremely sensitive to the spatial overlapping of the beam waists.

The maximum light intensity in the focal volume depends on the spatial distribution of intensity, but, in general, for a multimode laser beam this distribution may differ essentially from the one in a Gaussian beam. To get a correct value of light intensity the distribution of intensity in the focal region was measured by the method of a scanned knife edge [6,7]. A razor blade was driven by a precise translator across the beam in the focal plane of the objective or the mirror. The blade blocked a part of the laser beam and the fraction of the transmitted pulse energy was measured by a reference photodetector. For the laser wavelength near 500 nm the obtained data for the objective are shown in Fig. 2.

For a Gaussian beam the transmission function $F(x)$ has a well-known form [7]

$$F(x) = \int_{-\infty}^{x} \int_{-\infty}^{\infty} \exp\left(-\frac{x'^2 + y^2}{w^2}\right) dx'\, dy, \qquad (1)$$

where w is the radius of the beam to $1/e$ intensity level. A diffraction-limited Gaussian beam with the radius ρ on an aberration-free lens of the focal length f produces a focal spot with a $1/e$ radius of

$$w_0 = \frac{\lambda f}{2\pi\rho}. \qquad (2)$$

In our case the measured data can be approximated rather well by a transmission function determined by Eq. (1). This approximation gives the radius of the beam waist $w = 8$ μm, which is about 1.5 times larger than the w_0 determined by Eq. (2) for the same ρ (see Fig. 2). A similar result was obtained for the mirror where the $1/e$ radius of the beam waist was determined to be $w = 5$ μm.

The laser pulse measured by a coaxial phototube with a time resolution of about 2 ns is shown in Fig. 2. For the pulse peak power P the maximum light intensity I in the focal spot is given by the expression $I = P/\pi w^2$. Taking into account the losses on optical elements, the pulse energy of 2 mJ gives the maximum light intensity in the focus of 1×10^{11} W/cm^2 for the objective and 2×10^{11} W/cm^2 for the mirror. For excitation by counterpropagating beams the light intensity depends on the space-time overlapping of both beams. Comparative measurements of the breakdown threshold at different wavelengths have shown that in counterpropagating beams the intensity in the focal volume was increased by about 20–30 %.

The measurements of an intensity distribution by a scanned knife do not show the possible small-scale regions in the focus where the local intensity can essentially be increased. However, if such "hot spots" exist, the excitation conditions within the beam waist will be changed drastically. This question will be considered in more detail in the next section.

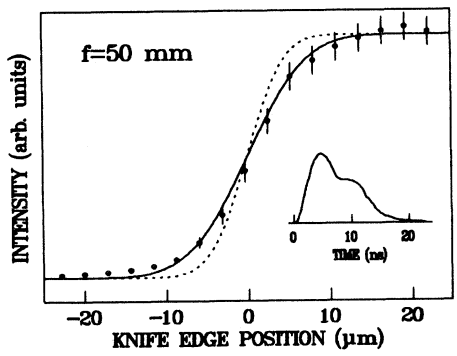

FIG. 2. Dependence of the transmitted pulse energy on the position of a knife edge in the beam waist: points, experimental data; solid curve, approximation by Eq. (1) with $w = 8$ μm; dotted curve, dependence for a diffraction-limited Gaussian beam with the same input diameter. The inset shows a typical laser pulse.

III. RESULTS AND DISCUSSION

A. Breakdown excitation spectra

The measurements of a selective breakdown were carried out in the 420–600 nm spectral region for xenon pressure of up to 2 bar. With the available laser pulse energy the breakdown of xenon could easily be initiated, which was observed as the appearance of a bright spark in the focus of the objective or the mirror. For the present experiments the most important factor was the dependence of the breakdown threshold on the laser wavelength. For some spectral regions the breakdown could be obtained at a very low pressure (several tens of torr), while for the other regions the breakdown initiation needed the gas pressure and/or the laser pulse energy to be essentially increased. The intensity of the laser spark shows similar variations with respect to the laser wavelength. A bright stable spark was induced by every laser pulse at some wavelengths, but only a weak unstable emission, if any, was observed when the laser was slightly tuned to the blue or to the red side. Therefore, the plots of spark intensity over the dye laser scans show a number of distinct resonances. The width of these resonances, where

the breakdown is easily induced, can be rather narrow (a few angstroms) and under proper excitation conditions the selective breakdown can even serve for a wavelength calibration. The appearance of a bright spark under on-resonance excitation allows one to carry out such a calibration without any measuring devices.

Figures 3–5 show typical breakdown excitation spectra obtained with three different laser dyes. In this spectral region the wavelength λ=511 nm corresponds to the five-photon ionization threshold for xenon, where the energy of laser photons makes one-fifth of the ionization potential of xenon V_{IP}=12.13 eV. To the blue side from this wavelength up to λ=409 nm the ionization of xenon proceeds by the absorption of at least five laser photons, while to the red side up to λ=613 nm six laser photons are required to ionize xenon atoms.

In the region of a five-photon ionization of xenon a number of four-photon atomic resonances can be recognized in the spectra (see Figs. 3 and 4). The positions of the corresponding atomic states in one-photon scale are marked in the figures. Some of the resonances have a broad diffuse background which is caused by molecular absorption. With an elevated gas pressure and/or an increased pulse energy, the molecular bands become more intensive and the selectivity of the breakdown gradually disappears. The atomic resonances are less sensitive to gas pressure and pulse energy; therefore, by variations of the excitation conditions one can get different relative intensities of atomic resonances and molecular bands in the spectra.

Near the five-photon ionization threshold both four- and five-photon atomic resonances are detected (see Fig. 4). Four-photon resonances correspond to the excitation of the lowest p states of xenon. For these intense resonances the breakdown threshold is several times lower than for any of the neighboring atomic resonances. The small peak near 502 nm is known from two-photon experiments [8,9] and it was attributed to a collision-induced excitation near the avoided crossing of the molecular potentials of $5d[\frac{1}{2}]_1$ and $6p[\frac{3}{2}]_1$ states [9].

To the red side from the five-photon ionization threshold two distinct progressions of five-photon atomic resonances are detected (see Figs. 4 and 5). The progression of the most intensive resonances results from the five-photon excitation of $nd[\frac{5}{2}]_3$ and $nd[\frac{7}{2}]_3$ states. For the measured spectral region the members of this progression start from the principal quantum number $n = 6$ and the peaks of d states can be traced in spectra up to n=16. At xenon pressure of 2 bar the $nd[\frac{5}{2}]_3$ and $nd[\frac{7}{2}]_3$ states are detected separately up to $n = 8$, where the energy difference between the states is 80 cm^{-1} [10]. In a one-photon scale this gives the spectral resolution of 16 cm^{-1} for the present conditions.

The progression of less intensive resonances belongs to $ns[\frac{3}{2}]_1$ states. Within the measured spectral region the five-photon excitation of the ns state starts from $n = 7$. However, in contrast to the states with $J = 3$, the lowest members of the ns progression are not detected in the spectra if the excitation is carried out by a single-pass laser beam. To observe the lowest ns resonances the counterpropagating excitation geometry should be used. Similarly, the peaks of some other atomic states with $J = 1$ are absent in the spectra for a unidirectional excitation geometry, but they are well pronounced if the excitation is performed by counterpropagating beams. These interesting phenomena will be considered below.

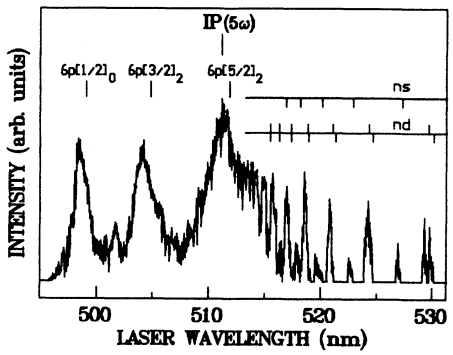

FIG. 4. Breakdown excitation spectrum near the five-photon ionization threshold. Xenon pressure, 2 bar; pulse energy, 0.8 mJ; counterpropagating excitation geometry.

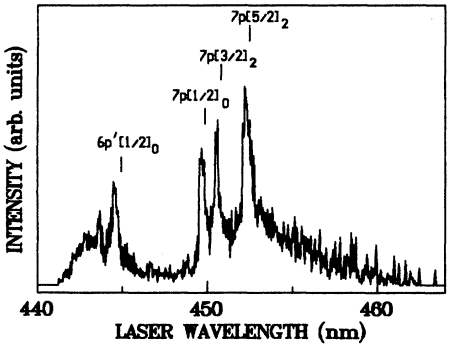

FIG. 3. Breakdown excitation spectrum in the region of four-photon p resonances. Xenon pressure, 1.8 bar; pulse energy, 1 mJ; unidirectional excitation by the spherical mirror.

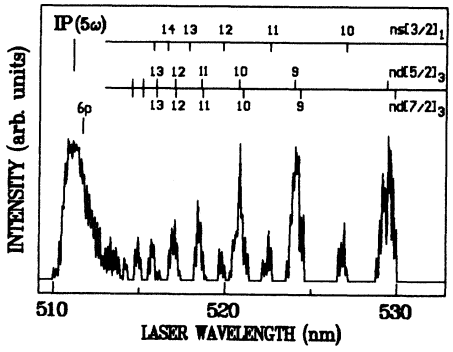

FIG. 5. Breakdown excitation spectrum below the five-photon ionization threshold. Xenon pressure, 2 bar; pulse energy, 0.8 mJ; unidirectional excitation by the objective.

Most of the atomic resonances in the spectra have an asymmetric profile, which is typical of REMPI in conditions of the ac Stark shift of atomic levels in a multimode laser pulse [11–13]. The range of ac Stark shifts in a multimode pulse determines the width of resonances, which is of the order of 10 cm^{-1} in a one-photon scale for the present experiments. The Stark broadening by free electrons for the initial stage of the breakdown is negligible [14].

In REMPI experiments the ac Stark shift of resonances provides a probe of the intensity in the focal region [11–13]. In the same manner the ac Stark shift of the resonances in the breakdown excitation spectra allows one to measure the light intensity in the focal volume and to determine the conditions of REMPI which initiate the breakdown. Figure 6 shows the breakdown excitation spectra measured near the three-photon resonance with the $6s[\frac{3}{2}]_1$ state. Again, a number of atomic and molecular resonances can be identified in the spectra. Under single-pass excitation the $6s$ resonance is not detected, but it can be seen clearly in the case of a counterpropagating excitation geometry. The maximum of the $6s$ resonance is shifted by about 0.4 nm to the blue side from the unperturbed position. The pressure-induced shift of this resonance is about 0.02 nm at 1 bar [15]. By using the value of the ac Stark shift constant $\alpha_\lambda = 0.0028$ nm GW^{-1} cm^2, reported in Ref. [11], the shift of the $6s$ resonance corresponds to the light intensity of 1.4×10^{11} W/cm^2. This value coincides well with the one obtained from the measurements of intensity by a scanned knife edge. It means that the initiation of the breakdown proceeds in the conditions of a smooth distribution of light intensity in the beam waist without hot spots with high local intensities.

In contrast to narrow asymmetric five-photon resonances, the four-photon $6p$ resonances are much broader and they have rather symmetrical Lorentzian-like contours (see Fig. 4). In the breakdown excitation spectra of krypton a similar broadening of the lowest $5p$ resonances has been observed [16]. Two-photon experiments [8,9] suggest that for the xenon pressure used, the broadening of $6p$ resonances is not caused by molecular absorption. For other four-photon resonances such broadening is absent, though these resonances have broad blue and red wings (see Figs. 3 and 6). In a one-photon scale the width of the $6p$ resonances is up to 100 cm^{-1} and this value is too large to be caused by the ac Stark effect or by the ionization broadening of the resonance state. For the photoionization cross section of 10^{-17} cm^2 [17,18] and the light intensity of 10^{11} W/cm^2 the ionization width of the $6p$ states is about 10 cm^{-1}, which corresponds to a few cm^{-1} in the one-photon scale for a four-photon excitation process. One can believe that, besides the REMPI via $6p$ states, the breakdown in this spectral region is initiated by other excitation processes which give an anomalous broadening of the corresponding resonances in the spectra. For a five-photon ionization such an additional excitation channel can be provided by an internally generated fifth-harmonic field, when xenon atoms are ionized by one-photon absorption of harmonic photons. In this case the nonlinear susceptibility $\chi^{(5)}$ is resonantly enhanced near the four-photon resonances with $6p$ states and the ionization by the fifth harmonic leads to the broadening of the corresponding peaks. The role of an internally generated harmonic field in the breakdown initiation will be discussed in more detail in Sec. III B.

When considering the spectra of a selective breakdown, it should be kept in mind that the breakdown can be initiated by the ionization of some uncontrolled impurities, especially if the ionization potential of these impurity atoms or molecules is lower than that of the bulk gas. At low concentrations impurities have no influence on the avalanche stage of the breakdown, but their role at the initial stage of the multiphoton ionization can be very important. In the breakdown spectra of krypton the most intensive atomic resonances of xenon [16] have always been detected; in the spectra of argon, the resonances of xenon and krypton, etc. For the present experiments with xenon the influence of impurities was checked by using the molecular chlorine, which has a very low breakdown threshold [19].

The influence of chlorine impurity is illustrated in Fig. 7. Small additions of chlorine reduce essentially the

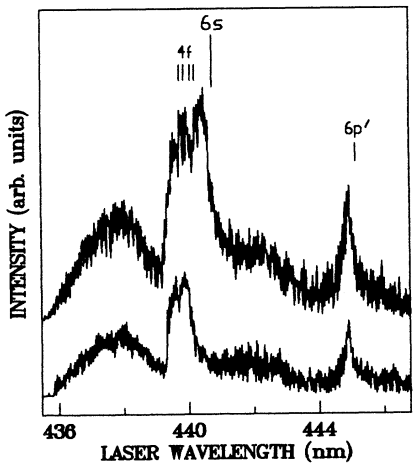

FIG. 6. Breakdown excitation spectrum near the three-photon $6s$ resonance. Upper trace, counterpropagating excitation geometry; lower trace, unidirectional excitation by the objective. Xenon pressure, 1 bar; pulse energy, 0.85 mJ.

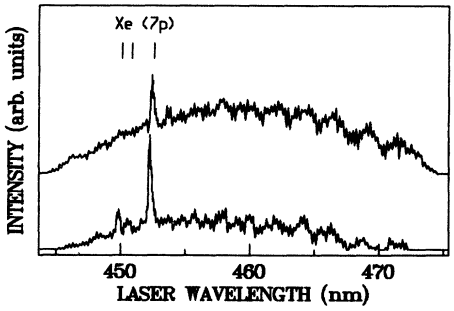

FIG. 7. Influence of chlorine addition on the spectra of the selective breakdown: upper trace, 1000 ppm of chlorine; lower trace, 300 ppm of chlorine. Xenon pressure, 1.2 bar; pulse energy, 0.6 mJ. Single-pass excitation by the mirror.

breakdown threshold and the atomic resonances of xenon in the spectra totally disappear. The breakdown becomes nonresonant and the intensity of the laser spark follows the variations of the laser output over the scan. If the content of chlorine in xenon is about 1000 ppm or less, the most intensive resonances of xenon appear in the spectra on the chlorine background. In this case a blurred structure can be seen in the background, where weak peaks are separated by about 120 cm^{-1}. This structure is probably caused by REMPI via vibronic levels of chlorine molecular states. For concentrations less than 100 ppm the chlorine background disappears and the spectra are identical to the case of pure xenon. Therefore, the level of about 100 ppm determines the concentration of molecular impurities, which can influence the measured spectra for the present excitation conditions. The concentration of impurities in xenon used was about an order of magnitude smaller.

B. Role of internal harmonic field

In general, a selective breakdown is induced due to REMPI via atomic and molecular excited states and a reduced breakdown threshold could be predicted for the wavelengths corresponding to allowed multiphoton transitions. However, for some of the odd-photon atomic resonances, in quite a broad range of excitation conditions, there was no evidence for the breakdown at the corresponding wavelengths when the laser beam was focused by either the objective or the mirror. Even in the case that the breakdown was induced, the spectra showed that it was caused by the wings of the neighboring resonances. The situation changed, however, when excitation was carried out by counterpropagating beams. The breakdown at the same wavelengths was easily initiated and well-pronounced intense resonances appeared in the spectra. In other words, the breakdown threshold for some wavelengths depends essentially on the excitation geometry and a high threshold for a single-pass excitation is reduced drastically for counterpropagating laser beams.

Similar effects are well known in REMPI spectra of rare gases, where some of the multiphoton atomic resonances are gradually reduced and totally disappear with the increased gas density. These resonances reappear, however, in spectra when the counterpropagating laser beams are used. Since 1977, when the suppression of multiphoton excitation was first observed [20,21], the cancellation of multiphoton resonances has been the object of extensive investigations [22–29]. The explanation of resonant suppression has been obtained by considering the cooperative response of the atomic system under excitation [23,30–35]. For certain excitation conditions atoms interact with the laser field not independently, but cooperative interaction becomes significant and the cooperative response of the atomic system can either suppress or facilitate ionization. For the states that can be excited by both one photon and q photons, where $q > 1$ is odd, a coherent field at the sum frequency can be generated under on-resonance excitation. Destructive interference between two excitation pathways, where the first one is a q-photon absorption from the laser field and the second is one-photon absorption of harmonic photons, is able to suppress REMPI and the corresponding q-photon resonance is canceled. For a counterpropagating excitation geometry no harmonic field is generated if at least one of the absorbed q photons is traveling opposite the other photons. Then the q-photon absorption becomes significant and the corresponding resonances reappear in the spectrum. All these effects were studied through direct ionization measurements, while in the present experiments they were observed through the initiation of a breakdown in a dense gas.

The cancellation of the three-photon $6s$ resonance in a breakdown is shown in Fig. 6. Under excitation by a unidirectional laser beam the $6s$ resonance is absent in the spectrum, but it appears under excitation by counterpropagating beams. A similar cancellation of five-photon resonances by six-wave mixing interference has been studied by REMPI in [26] and Fig. 8 shows how this effect is manifested in breakdown excitation spectra. For counterpropagating laser beams the five-photon resonance with the $7s[\frac{3}{2}]_1$ state is the most intensive one at any pulse energy when the breakdown takes place. It means that the breakdown threshold at this wavelength is the lowest for this spectral region. In a single-pass geometry, however, this resonance is absent and it is not observed even at an increased pulse energy when all other weak resonances are clearly seen. The peak near $\lambda = 587.5$ nm is known from the ionization spectra of xenon [26], where it was assigned to the ionization by the internally generated fifth-harmonic field.

Figure 9 shows a group of other five-photon resonances, where the cancellation effect was observed. Again, under the excitation by a unidirectional beam $8s[\frac{3}{2}]_1$ and $6d[\frac{3}{2}]_1$ resonances are not detected, but they are clearly seen under excitation by counterpropagating beams. For other $6d$ states with $J = 3$, one-photon transitions to the ground state are forbidden; therefore, the excitation of these states is not affected by the harmonic field and both these resonances are well pronounced for any excitation geometry.

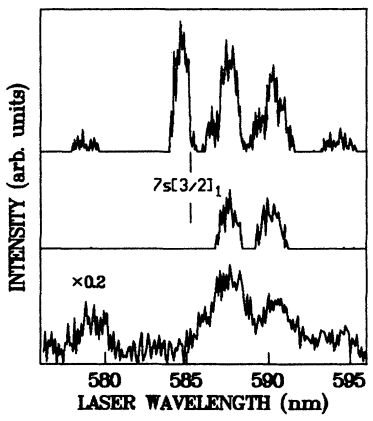

FIG. 8. Cancellation of the five-photon $7s$ resonance in the breakdown excitation spectra (from top to bottom): counterpropagating excitation (1.3 mJ); unidirectional excitation (1.3 mJ); unidirectional excitation (1.8 mJ). Xenon pressure, 2 bar.

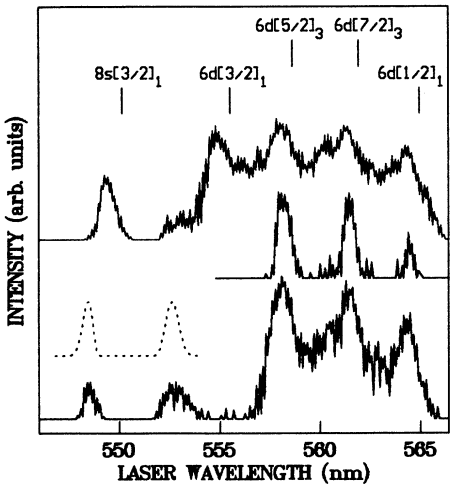

FIG. 9. Five-photon resonances and fifth-harmonic peaks in the breakdown excitation spectra (from top to bottom): counterpropagating excitation (1.2 mJ); unidirectional excitation (1.2 mJ); unidirectional excitation (1.5 mJ). Xenon pressure, 2 bar. The dotted line shows the calculated phase-matching curves for the fifth harmonic.

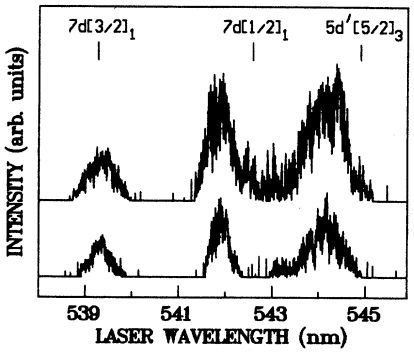

FIG. 10. Uncanceled five-photon resonances in the breakdown excitation spectra: upper trace, counterpropagating excitation; lower trace, unidirectional excitation. Xenon pressure, 2 bar; laser pulse energy, 1.4 mJ.

Formally, the excitation of the $6d[\frac{1}{2}]_1$ state (λ = 564 nm) could be influenced by the cancellation effect as well, but the corresponding resonance is clearly seen under unidirectional excitation. Moreover, $8s[\frac{3}{2}]_1$ is the highest excited state for which the cancellation effect in the breakdown excitation spectra was observed. Further towards the ionization limit, where a number of other five-photon resonances could be canceled (see Figs. 4 and 5), no evidence of the cancellation was detected. Figure 10 shows a group of five-photon resonances next from $8s[\frac{3}{2}]_1$ to the blue side. For the excitation of the $5d'[\frac{5}{2}]_3$ state the cancellation effect is absent, but for other two the $7d$ resonances this effect could be expected. Nevertheless, both of the $7d$ resonances can be seen in any excitation geometry. The introduction of the counterpropagating beam makes the resonances broader and more intensive, but this results from the increased intensity in the focal volume. The $5d'$ resonance shows a similar behavior and the relative intensities of all peaks remain nearly the same.

As it will be discussed below, near the five-photon s and d resonances, having J =1, an additional ionization peak can be detected. This peak is caused by the internally generated fifth-harmonic field and for higher excited states, where the negatively dispersive region is rather narrow, the harmonic peak is located very close to the atomic resonance. Thus, for a single-pass excitation geometry the excitation profiles detected near the atomic resonances could be provided by the fifth harmonic, while the atomic resonance is suppressed by the cancellation effect. In this case, however, the excitation by counterpropagating beams should result in the appearance of an atomic resonance which is more intensive and, for higher excited states, broader than the corresponding harmonic peak. In the present experiments, all the uncanceled s and d resonances are detected indeed as "normal" atomic resonances and not as narrow and less intensive harmonic peaks.

The condition whether a resonance is canceled or not depends on the resonant and nonresonant components of the phase mismatch under on-resonance excitation [31,34,36,37]. For a dense gas, where pressure-induced broadening dominates, and neglecting the ac Stark effect, this condition in a plane-wave approximation can be written in the form [34]

$$|\kappa/\Delta k_0| \gg \Gamma_c \tag{3}$$

where Γ_c is the pressure-induced width and Δk_0 is the nonresonant contribution to the phase mismatch. The parameter κ determines the resonant component of the phase mismatch κ/Δ_r, where Δ_r is the detuning from the resonance. The value of κ is proportional to the atomic number density N and the oscillator strength f_i for the ith atomic resonance:

$$\kappa = (\pi e^2/mc) N f_i. \tag{4}$$

Conditions (3) and (4) allow one to consider qualitatively the cancellation of resonances. The oscillator strengths for the transitions to the $6d[\frac{1}{2}]_1$ and $7d[\frac{3}{2}]_1$ states of xenon are small ($f_i < 0.001$ [38]) and due to the nonresonant contribution from the neighboring off-resonance levels the corresponding five-photon resonances remain uncanceled (see Figs. 9 and 10).

A more interesting example is the cancellation of $8s[\frac{3}{2}]_1$ and $7d[\frac{1}{2}]_1$ resonances. The transitions to these states have nearly equal oscillator strengths (0.0222 for $8s[\frac{3}{2}]_1$ and 0.0227 for $7d[\frac{1}{2}]_1$ [38]). Nevertheless, the $8s$ resonance shows a well-pronounced cancellation effect, while $7d$ resonance remains uncanceled. Equal oscillator strengths for the corresponding transitions give equal resonant components of the phase mismatch for on-resonance excitation. Thus the different behavior of the resonances results from nonresonant components of the phase mismatch. The observed cancellation of the $8s[\frac{3}{2}]_1$ resonance means that the nonresonant contribution from other off-resonance levels is rather small and

the residual uncanceled peak is weak enough. For the higher-lying $7d[\frac{1}{2}]_1$ state the off-resonance levels are located closer and they give a large nonresonant contribution to the phase mismatch, especially for a high gas density when the pressure-induced broadening is significant. In this case the interference between the excitation pathways is incomplete and the corresponding resonance remains uncanceled. Similarly, for the next excited states the oscillator strengths f_i decrease and the close location of these states to each other gives a large nonresonant contribution to the phase mismatch. This makes the corresponding resonances uncanceled.

The observation of the cancellation effect in a laser-induced breakdown presents direct evidence of the role of an internally generated harmonic field in the breakdown initiation. Moreover, the selective breakdown is a very impressive demonstration of a cancellation, caused by destructive interference between optical transitions. For the canceled resonances a bright spark arises in the focal region at the counterpropagating excitation geometry, but this spark disappears totally when the reflecting mirror is blocked or slightly tilted.

In the case of on-resonance excitation the harmonic field is able to suppress REMPI and prevent the initiation of the breakdown. Besides, under certain conditions the harmonic field can produce an additional ionization [22,26,35]. The initiation of a breakdown is very sensitive to any of the ionization processes in the focal volume and the appearance of additional ionization channels should remarkably reduce the breakdown threshold. In a dense gas, however, the generated harmonic photons can hardly be detected directly because of strong absorption. Nevertheless, even a low-efficiency generation of harmonics in the focal region will drastically change the excitation conditions due to a number of effective ionization channels where harmonic photons are involved [22,23,31,35].

As discussed in Sec. III A, the anomalous broadening of some of the four-photon resonances may be caused by the fifth-harmonic field. Besides, the phase-matched fifth harmonic can be generated in a negatively dispersive region near atomic five-photon resonances. As a rule, the canceled five-photon resonances in breakdown excitation spectra are accompanied from the blue side by resonancelike peaks (see Figs. 8 and 9). All these peaks are absent if the excitation is carried out by circularly polarized light. With the increase of the xenon pressure the peaks are shifted to the blue side away from the resonance. If, however, a foreign gas is added (argon or krypton), the peaks are registered closer to the resonance. All these properties argue for the nature of the peaks to be of an internally generated fifth-harmonic field origin similar to the peak near $\lambda = 587.5$ nm [26].

The spectral dependence of the intensity of the fifth harmonic can be calculated by using the well-known formalism [39]. This dependence is determined by the phase-matching integral and for a focused Gaussian beam it is given by the expression

$$|F(b\Delta k)|^2 = \begin{cases} \frac{\pi^2}{576}(b\Delta k)^6 \exp(b\Delta k), & \Delta k < 0 \\ 0, & \Delta k > 0 \ , \end{cases} \tag{5}$$

where $\Delta k = k_5 - 5k_1$ is the phase mismatch, and $b = 4\pi w^2/\lambda$ is the confocal parameter of the Gaussian beam. To calculate the refractive indices at a wavelength λ the Sellmeir formula was used:

$$n(\lambda) - 1 = \frac{Nr_e}{2\pi} \sum_i \frac{f_i}{\lambda_i^{-2} - \lambda^{-2}}, \tag{6}$$

where $r_e = 2.818 \times 10^{-13}$ cm, N is the atomic number density, and f_i is the oscillator strength for the ith transition at the wavelength λ_i. The data about f_i were taken from Ref. [38]. For the measured w the confocal parameter b near 550 nm was 1.3 mm and 0.6 mm for the objective and the mirror, respectively.

The calculated phase-matching curves for the conditions of the experiment are shown in Fig. 9. In a focused Gaussian beam the maximum of the fifth harmonic corresponds to $b\Delta k = -6$ and the calculated curves coincide well with the harmonic peaks despite the neglect of absorption and the ac Stark effect in the calculations. The presence of such resonancelike peaks in the spectra means a remarkable lowering of the breakdown threshold at the corresponding wavelengths in contrast to an on-resonance excitation, where the harmonic field can suppress REMPI and enhance the breakdown threshold.

The generation of harmonics in the focal region influences essentially the initiation of the breakdown and this circumstance should always be kept in mind when interpreting the experimental results. The harmonic field, even though not detected directly, may be responsible for a number of anomalous phenomena associated with the breakdown. These phenomena have been known since the earliest investigations of laser-induced breakdown, but they still remain without satisfactory explanations.

One group of such phenomena is formed by the results of the measurements of the breakdown threshold for different focal-length lenses [40–45]. With a tighter focusing the breakdown threshold often increases, but this increase is difficult to explain considering the diffusion of electrons, diffusionlike losses in the focal volume, or other reasons [41,46,47]. As a tentative explanation, the diffusion losses from small-scale hot spots have been suggested to be responsible for the increase of the threshold [46,47]. However, similar results were obtained with single-mode lasers [42–44], which give a smooth intensity distribution in the focal spot. The present experiments have not shown the existence of hot spots either.

The variations of the breakdown threshold, however, are explained qualitatively by taking into account the additional ionization by an internally generated harmonic field. The intensity of the harmonic field depends on the phase-matching parameter $b\Delta k$ and the variations of the focal length influence the phase matching through the variations of the confocal parameter b. In this case the rise of the threshold reflects the decrease of the number of the harmonic photons generated in the focal volume. Some similarity can be found in Ref. [48], where the number of harmonic photons for a tightly focused beam has been determined to be proportional to b^3.

Other interesting results have been obtained in the experiments with gas mixtures [41,47]. Surprisingly, the breakdown threshold for the mixture of argon and neon

is reduced by several times with respect to the thresholds for pure argon or pure neon. This was observed by using a neodymium laser, but the effect was absent if a ruby laser was used [47]. These results have remained unexplained, as none of the considered reasons (diffusionlike losses, the Penning reaction, etc.) can be responsible for the observed phenomena. However, all these effects are explainable considering the harmonic field. The use of gas mixtures is a well-known method of phase matching, when one of the mixture components is a negatively dispersive active gas and another component is a positively dispersive buffer gas. One can suggest that for the wavelength of a neodymium laser the mixture of argon and neon improves the phase matching through the variations of Δk and, as a result, the generated harmonic field reduces the breakdown threshold.

IV. CONCLUSION

The experiments with laser-induced breakdown in xenon have shown that the breakdown excitation spectra are very similar to the common REMPI spectra, where the ionization yield is measured. All the channels of REMPI and the associated processes, including quite fine effects, can be reproduced well and visualized by the laser spark. Therefore, the excitation of a selective breakdown can serve as a very simple and effective method for the study of multiphoton processes in dense gases. Moreover, measuring the bright broadband emission of the laser spark is often much easier than measuring an ionization yield.

At a light intensity of 10^{11} W/cm^2 and xenon pressure of 1–2 bar the breakdown in the spectral range of 420–600 nm is induced selectively. This selectivity is provided by REMPI via excited atomic and molecular states of xenon. A number of three-, four-, and five-photon resonances have been identified in breakdown excitation spectra. The influence of impurities on the measured spectra has been checked by adding molecular chlorine, and a level of about 100 ppm for the chlorine concentration has been estimated to influence the initiation of a breakdown.

Due to the selectivity of the breakdown, the excitation conditions in the focal volume can be determined from the ac Stark shift of the resonances. The measurements have shown that for the present experiments the initiation of the breakdown proceeds under the conditions of a smooth distribution of light intensity in the beam waist without of hot spots with high local intensities.

An essential role of the internally generated harmonic field in the initiation of a breakdown has been established. These results agree well with the previous investigations of multiphoton excitation and ionization of rare gases. The harmonic photons generated in the focal volume can both initiate or suppress the breakdown, depending on the laser wavelength. The phase-matched harmonic field is generated at the high-energy side of the resonances allowed for a one-photon transition to the ground state. Similarly, the harmonic field can be generated under odd-photon excitation to the continuum, when nonlinear susceptibility is resonantly enhanced near intermediate atomic resonances. In these cases harmonic photons produce an additional ionization and reduce significantly the breakdown threshold. However, for some of the atomic resonances the generated harmonic field and the interference between optical transitions suppress REMPI and prevent the initiation of the breakdown. This cancellation effect is actual for an excitation by a single-pass laser beam. For a counterpropagating excitation geometry, when the cancellation effect is partially spoiled, the breakdown threshold for the same wavelengths is drastically reduced. It has been shown that for the present experimental conditions the cancellation effect is well pronounced for the lowest s and d states of xenon, having $J=1$, while this effect is not observed under the excitation of the higher-lying states. One can suppose that the harmonics of the laser field are responsible for some effects known from previous experiments on the laser-induced breakdown. A qualitative explanation of some of these effects has been suggested.

ACKNOWLEDGMENTS

This work was supported by the Estonian Science Foundation (Grant No. 945) and by Soros Foundation Grant, given by the American Physical Society.

[1] T. P. Hughes, in *Physics of Quantum Electronics,* edited by P. Kelly *et al.* (McGraw-Hill, New York, 1966), p. 200.
[2] Yu. P. Raizer, *Laser Induced Discharge Phenomena* (Consultants Bureau, New York, 1977).
[3] G. M. Weyl, in *Laser-Induced Plasmas and Applications,* edited by L. Radziemski and D. Cremers (Dekker, New York, 1989), p. 1.
[4] H. T. Busher, R. G. Tomlinson, and E. K. Damon, Phys. Rev. Lett. **15**, 847 (1965).
[5] N. Damany, P. Laporte, J.-L. Subtil, and H. Damany, Phys. Rev. A **32**, 3418 (1985).
[6] D. R. Skinner and R. E. Witcher, J. Phys. E **5**, 237 (1972).
[7] W. L. Smith, J. H. Bechtel, and N. Bloembergen, Phys. Rev. B **12**, 706 (1975).
[8] W. Gornik, S. Kindt, E. Matthias, and D. Schmidt, J. Chem. Phys. **75**, 68 (1981).
[9] T. D. Raymond, N. Böwering, Chien-Yu Kuo, and J. W. Keto, Phys. Rev. A **29**, 721 (1984).
[10] C. E. Moore, *Atomic Energy Levels,* Natl. Bur. Stand. (U.S.) Circ. No. 467 (U.S. GPO, Washington, DC, 1958), Vol. III.
[11] P. Kruit, J. Kimman, H. G. Muller, and M. J. Van der Wiel, J. Phys. B **16**, 937 (1983).
[12] L. Li, B.-X. Yang, and P. M. Johnson, J. Opt. Soc. Am. B **2**, 748 (1985).
[13] S. Xu, G. Sha, J. He, and C. Zhang, J. Chem. Phys. **100**, 1866 (1994).

[14] Truong-Bach, J. Richou, A. Lesage, and M. H. Miller, Phys. Rev. A **24**, 2550 (1981).
[15] W. R. Ferrell, M. G. Payne, and W. R. Garrett, Phys. Rev. A **36**, 81 (1987).
[16] V. E. Peet (unpublished).
[17] C. Duzy and H. A. Hyman, Phys. Rev. A **22**, 1878 (1980).
[18] M. S. Pindzola, Phys. Rev. A **23**, 201 (1981).
[19] J. A. Howe, J. Appl. Phys. **36**, 3363 (1965).
[20] K. Aron and P. M. Johnson, J. Chem. Phys. **67**, 5099 (1977).
[21] F. H. M. Faisal, R. Wallenstein, and H. Zacharias, Phys. Rev. Lett. **39**, 1138 (1977).
[22] J. C. Miller, R. N. Compton, M. G. Payne, and W. R. Garrett, Phys. Rev. Lett. **45**, 114 (1980); J. C. Miller and R. N. Compton, Phys. Rev. A **25**, 2056 (1982).
[23] D. J. Jackson and J. J. Wynne, Phys. Rev. Lett. **49**, 543 (1982); D. J. Jackson, J. J. Wynne, and P. H. Kes, Phys. Rev. A **28**, 781 (1983).
[24] J. H. Glownia and R. K. Sander, Phys. Rev. Lett. **49**, 21 (1982).
[25] R. N. Compton and J. C. Miller, J. Opt. Soc. Am. B **2**, 355 (1985).
[26] W. R. Garrett, S. D. Henderson, and M. G. Payne, Phys. Rev. A **35**, 5032 (1987).
[27] P. R. Blazewicz and J. C. Miller, Phys. Rev. A **38**, 2863 (1988).
[28] D. Charalambidis, X. Xing, J. Petrakis, and C. Fotakis, Phys. Rev. A **44**, R24 (1991).
[29] X. Xing, D. Charalambidis, E. Koutsourelaki, and C. Fotakis, Phys. Rev. A **47**, 2296 (1993).
[30] M. G. Payne, W. R. Garrett, and H. C. Baker, Chem. Phys. Lett. **75**, 468 (1980).
[31] M. G. Payne and W. R. Garrett, Phys. Rev. A **26**, 356 (1982); **28**, 3409 (1983).
[32] M. Poirier, Phys. Rev. A **27**, 934 (1983).
[33] J. J. Wynne, Phys. Rev. Lett. **52**, 751 (1984).
[34] M. G. Payne, W. R. Garrett, and W. R. Ferrell, Phys. Rev. A **34**, 1143 (1986).
[35] W. R. Garrett, W. R. Ferrell, M. G. Payne, and J. C. Miller, Phys. Rev. A **34**, 5032 (1986).
[36] S. P. Tewari and G. S. Agarwal, Phys. Rev. Lett. **56**, 1811 (1986).
[37] M. Elk, P. Lambropoulos, and X. Tang, Phys. Rev. A **44**, R31 (1991).
[38] W. F. Chan, G. Cooper, X. Guo, G. R. Burton, and C. E. Brion, Phys. Rev. A **46**, 149 (1992).
[39] J. F. Reintjes, *Nonlinear Optical Parametric Processes in Liquids and Gases* (Academic, New York, 1984).
[40] A. F. Haught, R. G. Meyerand, and D. C. Smith, in *Physics of Quantum Electronics* (Ref. [1]), p. 509.
[41] D. C. Smith and A. F. Haught, Phys. Rev. Lett. **16**, 1085 (1966).
[42] M. Young and M. Hercher, J. Appl. Phys. **38**, 4393 (1967).
[43] D. C. Smith and R. G. Tomlinson, Appl. Phys. Lett. **11**, 73 (1967).
[44] A. J. Alcock, C. De Michelis, and M. C. Richardson, IEEE J. Quantum Electron. **QE-6**, 622 (1970).
[45] S. A. Batishche *et al.*, Zh. Tekh. Fiz. **57**, 2418 (1987) [Sov. Phys. Tech. Phys. **32**, 1470 (1987)].
[46] Ya. B. Zel'dovich and Yu. P. Raizer, Zh. Eksp. Teor. Fiz. **47**, 1150 (1964) [Sov. Phys. JETP **20**, 772 (1965)].
[47] B. F. Mul'chenko and Yu. P. Raizer, Zh. Eksp. Teor. Fiz. **60**, 643 (1971) [Sov. Phys. JETP **33**, 272 (1972)].
[48] L. A. Lomprè *et al.*, J. Opt. Soc. Am. B **7**, 754 (1990).